



# APPLICATION OF ORTHOGONAL CURVILINEAR MESHES TO THE TLM METHOD

H. Meliani<sup>1</sup>, and Y.A. Jebbar<sup>2</sup>

1:Lecturer, College of Technology at El-Ahsa, KSA

2:Senior Engineer, Electronic Department, University of Blida, Algeria.

E-mail: melianih@hotmail.com.

## ABSTRACT

*In this article, orthogonal curvilinear meshes described by [Meliani, H, 1988] and [Meliani, H. et al, 2000], are applied to the TLM method. To this end, the symmetrical super condensed node (SSCN) described by [Trenkic, V et al, 1995] is used. To validate our results, two types of cavities are studied. The resonant frequency of the dominant modes is calculated. The obtained results are compared to the analytical results and to the results given by cartesian meshes in [Trenkic, V et al, 1995] and [Akhtarzad, S et al, 1975].*

**Keywords:** TLM, Curvilinear, mesh, cavities, resonant frequency, electromagnetic field.

[Meliani, H, 1988]

.TLM

(SSCN)

[Meliani, H. et al, 2000]

.[Trenkic, V et al, 1995] (SSCN)

[Trenkic, V et al, 1995]

.[Akhtarzad, S et al, 1975]

## 1. INTRODUCTION

Over the last few years, the TLM method has been used to solve a variety of problems [Christopoulos, C., 1995] such as: two-dimensional scattering problems in rectangular waveguides, Two-dimensional eigenvalue and hybrid field problems, three-dimensional eigenvalue and hybrid field problems, diffusion problems, vibration and acoustics, electromagnetic compatibility, microwave design, radar cross-section (RSC), antennas, and

electromagnetic heating. In [Christopoulos, C., 1995] the theory and application of the TLM method as applied to these problems are well presented. The author gives a large variety of references related to the TLM method.

Since its advent, the TLM method has always been used with a cartesian mesh to solve a variety of problems stated above [Christopoulos, C., 1995] and [Akhtarzad, S et al, 1975]. At first, uniform cartesian meshes were used and they were perfectly adapted to problems with regular boundaries. However for problems with irregular boundaries or singularities where the gradient of the field is high, the meshes need to be fine in these areas. For this type of problems regular meshes are not suitable because the number of the nodes to be used can be excessive which demand large storage capacity and execution time. So irregular cartesian meshes were used and made fine in the regions where the gradient of the field is high [Al-Mukhtar, D. A. et al, 1981], [Saguet, P. et al]. The inconvenience of the Cartesian meshes is that they do not describe the boundaries correctly. The development of variable or graded meshes [Al – Mukhtar, D. A. et al, 1981] has made possible modeling in a non-cartesian mesh. Following this development, a new approach was proposed in [Meliani, H., 1988], [Meliani, H., et al, 2000] which consists of the automatic generation of orthogonal curvilinear meshes in two and three dimensions.

The advantages of using a mesh other than cartesian is that:

- The curvilinear mesh fits the boundaries. This is important for the accuracy of modeling. A curved boundary would have to be described in a step-wise fashion if a rectangular grid is used.
- The mesh is orthogonal and automatically generated. This latter feature would overcome the burden of data preparation to describe the topology of the mesh especially in three dimensions.
- The mesh is crowded in an organized way around a point where there is a field singularity.
- Another advantage of a curvilinear mesh is that a saving in computer storage may be achieved.

However, orthogonal curvilinear meshes demand an effort of computation to generate them as is shown in [Meliani, H., 1988].

The similarities between curvilinear meshes and non-uniform cartesian meshes is that the analysis of a node in both meshes is the same. The main difference is that lengths of the lines in curvilinear meshes are curved whereas they are straight in cartesian meshes. This difference will have an influence in the values of the parameters (capacitance and inductance) of the node since they are function of length lines as it is shown in the following section.

To improve TLM method, new types of nodes have been used in three dimensions such as hybrid symmetrical condensed node (HSCN) and the symmetrical super condensed node (SSCN). These nodes have been used in non-uniform Cartesian mesh, and they yield substantial good results [Trenkic, V et al, 1995], [Christopoulos, C., 1995].

In this paper orthogonal curvilinear meshes are used in conjunction with the symmetrical super- condensed node in TLM to calculate resonant frequency of some practical electromagnetic field problems. The generated meshes are performed using Gauss surfaces as described in [Meliani, H, 1988] and [Meliani, H, et al, 2000]. To compare the effectiveness of orthogonal curvilinear meshes and non-uniform cartesian meshes, two examples studied in [Trenkic, V et al, 1995] and [Akhtarzad, S et al, 1975] are treated here. The examples are two resonant cavities for which the resonant frequencies of the dominant modes are calculated.

## 2. REPRESENTATION OF SSCN NODE

The theory of the SSCN TLM node in three dimensions is well described in [Trenkic, V et al, 1995]. For completeness, the results of this theory used in the work presented in this article are given in this section.

Figure1 represents a node of an orthogonal curvilinear mesh in three dimensions [Meliani, H, 1988] and figure 2 represents its TLM SSCN node. In the figures 1 and 2 below,  $\Delta l_1 = \Delta x$ ,  $\Delta l_2 = \Delta y$ ,  $\Delta l_3 = \Delta z$ .

The SSCN node is an amelioration of the hybrid node [Trenkic, V et al, 1995], [Christopoulos, C., 1995] in a sense that all the stubs are suppressed to diminish the scattering matrix, but the time step  $\Delta t$  is increased. A SSCN node comprises 12 ports as shown in figure2. Each two adjacent lines have the same characteristic impedance. The use of this type of node in conjunction with the orthogonal curvilinear mesh yields more precise results with less computing time and storage as will be seen in subsequent sections.

The computation and notation used with SSCN node with regard to figure2, is as follows [Trenkic, V et al, 1995]. This notation is adopted in the work presented in this article.

$V_{inj}$ : indicates the polarization potential  $j$ , in the propagation direction  $i$ . The subscript  $n$  indicates the position of  $V_{inj}$  with respect to the center of the node ( $n$  stands for negative).

$V_{ipj}$ : indicates the polarization potential  $j$ , in the propagation direction  $i$ . The subscript  $p$  indicates the position of  $V_{ipj}$  with respect to the center of the node ( $p$  stands for positive).

$C_{ij}$ : indicates the capacitance per unit length for the polarization wave  $j$ , in the propagation direction  $i$ .

$L_{ij}$ : indicates the inductance per unit length for the polarization wave  $j$ , in the propagation direction  $i$ .

$Z_{ij}$ : indicates the characteristic impedance of the polarization line  $j$ , in the propagation direction  $i$ .

$$V_1=V_{ynx}, V_2=V_{znx}, V_3=V_{xny}, V_4=V_{zny}, V_5=V_{ynz}, V_6=V_{xnz}, V_7=V_{ypz}, V_8=V_{zpy}, V_9=V_{zpx},$$

$$V_{10}=V_{xpz}, V_{11}=V_{xpy}, V_{12}=V_{ypx}.$$

The total capacitance and the total inductance in a given direction are as follows:

$$C_{ik} \Delta i + C_{jk} \Delta j = \epsilon \Delta i \Delta j / \Delta k \dots\dots\dots (1)$$

$$L_{ij} \Delta i + L_{ji} \Delta j = \mu \Delta i \Delta j / \Delta k \dots\dots\dots (2)$$

$i, j, k$  taking all the values  $x, y, z$  and  $i \neq j \neq k$

The time constant  $\Delta t$ , which must be constant along all the lines, is [Trenkic, V et al, 1995]:

$$\Delta t = \Delta i \sqrt{(C_{ij} L_{ij})} \dots\dots\dots (3)$$

and is taken as the smallest possible one.

The above 3 equations are solved in [Trenkic, V et al, 1995] to find the characteristic impedance of each line which is:

$$Z_{ij} = \Delta j \Delta \ell (\sqrt{\mu/\epsilon}) / [2c_{ij} \Delta i \Delta k] \dots\dots\dots (4)$$

Where

$$\Delta \ell = 2\Delta t / (\sqrt{\mu\epsilon}) \text{ for a cubic node of dimension } \Delta \ell.$$

$$c_{ij} = C_{ij} \Delta j / (\epsilon \Delta k) \dots\dots\dots (5)$$

$$\ell_{ij} = L_{ij} \Delta k / (\mu \Delta j) \dots\dots\dots (6)$$

The relations between the incident and reflected impulses are given by [Trenkic, V et al, 1995]:

$$V_{inj}^r = V_j + I_k Z_{ij} - V_{ipj}^i \dots\dots\dots (7)$$

$$V_{ipj}^r = V_j - I_k Z_{ij} - V_{inj}^i \dots\dots\dots (8)$$

Where

$$V_j = c_{ij}(V_{inj}^i + V_{ipj}^i) + c_{kj}(V_{knj}^i + V_{kpi}^i)$$

$$I_k = (\ell_{ij}/Z_{ij}) (V_{ipj}^i - V_{inj}^i + V_{jni}^i - V_{jpi}^i).$$

$V_j$  and  $I_k$  represent respectively the node voltage and current in the directions  $j$  and  $k$ .

The excitation of this type of node obeys to the same rule of the other type of nodes [Trenkic, V et al, 1995], [Christopoulos, C., 1995].

The excitation of the electric field  $E_j = -V_j/\Delta_j$  in the  $j$ -direction is done by taking:

$$V_{inj} = V_{ipj} = V_j/4c_{ij} \tag{9}$$

$$V_{knj} = V_{kpi} = V_j/4c_{kj} \tag{10}$$

The magnetic field  $H_k = I_k/\Delta_k$  is excited in same manner, i.e.

$$V_{ipj} = -V_{inj} = V_{jni} = -V_{jpi} = I_k Z_{ij}/4 \ell_{ij} = I_k Z_{ij}/4c_{ik} \tag{11}$$

Once all the parameters of a node are determined and the input and output nodes chosen, the conventional technique of TLM is used to solve a problem under consideration.

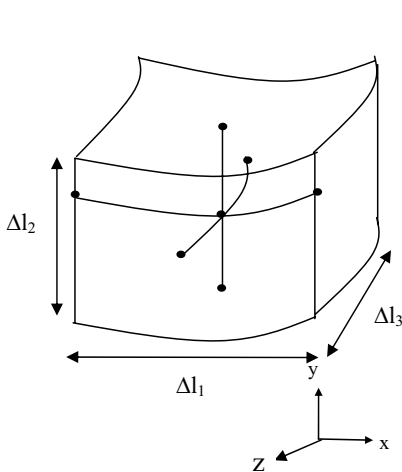


Figure.1 Node in three-dimensional orthogonal curvilinear mesh

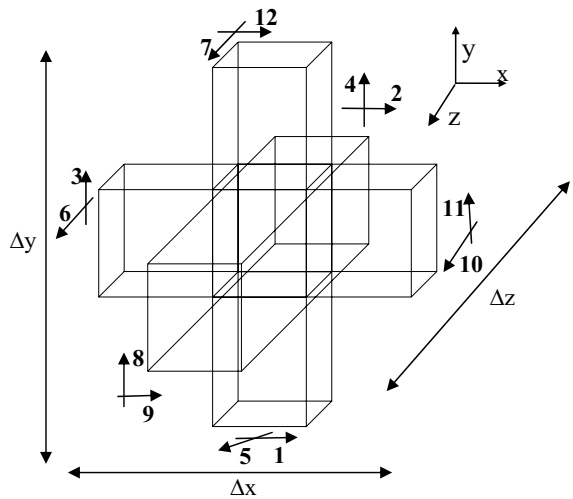


Figure.2 TLM SSCN node

### 3. FORM OF THE OUTPUT

The TLM output, in a given output node, consists of a stream of impulse functions for the particular field component under consideration [Johns, P.B. et al, 1971]. These impulses are of varying magnitude in the time domain and are separated by a time interval  $\Delta t$  seconds. For analysis purposes it is usual to take the Fourier transform of this function to yield the response to an excitation varying sinusoidally with time in a chosen input node. Since the output is in the form of a discrete series of delta functions, the Fourier transform integral equation (12), may be replaced by a summation thus yielding the real and imaginary parts of the output spectrum given by equations (13).

$$I(f) = \int_{-\infty}^{+\infty} I(t - n\Delta t) \exp(-j\omega t) dt \quad (12)$$

$$\text{Re}[F(\Delta l / \lambda)] = \sum_{K=1}^N I_K \cos(2\pi K \Delta l / \lambda)$$

$$\text{Im}[F(\Delta l / \lambda)] = \sum_{K=1}^N I_K \sin(2\pi K \Delta l / \lambda) \quad (13)$$

Where Re is the real part of the spectrum and Im is the imaginary part. N is the total number of iterations used  $I_K$  is the output amplitude at time  $t = K\Delta t$ .

The truncation of the output in the time domain (which is necessary for practical reasons) causes a spreading of the solution delta function into  $\sin(x)/x$  type of curves [Johns, P.B.,1972]. For greater resolution in the frequency domain sufficient number of iterations must be used to separate the solution points clearly and reduce error caused by time truncation of the output. Examples of this output will be given in subsequent sections.

### 4. APPLICATION OF THE METHOD TO TWO EXAMPLES

The orthogonal curvilinear mesh is used in this section to study two examples already analyzed with cartesian meshes in [Trenkic, V et al, 1995] and [Akhtarzad, S et al, 1975]. The results of the two techniques are then compared. The examples are:

- A cavity with two layers of dielectric which is analyzed in [Trenkic, V et al, 1995] using non-uniform cartesian meshes.
- A cavity with one layer of dielectric in the middle which is analyzed in [Akhtarzad, S et al, 1975] using uniform cartesian meshes and here using non-uniform meshes for comparison.

#### 4.1. Cavity With Two Layers Of Dielectrics: Dominant Mode TE<sub>110</sub>

The problem presented in this section is the cavity shown in figure3 studied in [Trenkic, V et al, 1995]. It contains two layers of dielectric ( $\epsilon_r = 4$ ). The resonant frequency of the dominant mode TE<sub>110</sub> is evaluated. The dimensions of the cavity are as follows as given in [Trenkic, V et al, 1995]:

Length =  $10a$ , width =  $a$ , dielectric width =  $a/4$ , gap between the two dielectrics =  $a/2$

For this problem there is no propagation in the  $z$ -direction, therefore one computing surface only is used in the  $z$ -direction with two extreme surfaces used as boundaries. The excitation is done in the  $z$ -direction. The input node is taken in one layer of dielectric whereas the output node is taken in the other layer.

Figure4 shows a sample of a surface generated in  $(x, y)$  plane with 10 nodes in the  $x$ -direction and 8 nodes in the  $y$ -direction. One can notice the curvature of the lines and the variation of their spacing in the dielectric layers and this is due to the presence of the dielectric.

Table 1 shows the results obtained for the resonant frequency of the dominant mode TE<sub>110</sub> for different types of meshes. One can notice that there is an appreciable improvement of the results obtained for the curvilinear meshes (Cv) with fewer nodes with regard to the Cartesian meshes. For instance, for a mesh of 60 nodes, the error of the result for the non-uniform cartesian mesh (CNU) is twice the error of the result of curvilinear mesh. The curvilinear mesh of 120 nodes gives an error, which is five times smaller than the error of the non-uniform mesh of 480 nodes. These results prove that curvilinear meshes permit savings in capacity storage and execution time. It is worth noting that, in the orthogonal curvilinear meshes the number of nodes ( $=10$ ) is kept constant outside the dielectric and varied inside the dielectric to have a concentration of nodes in this region.

An investigation has been made on the convergence to the theoretical value of the different numerical results. These are shown in figure5 that represents the variation of the frequency versus the number of nodes for the orthogonal curvilinear meshes and the non-uniform meshes. One can notice the rapid convergence to the theoretical result of the curvilinear mesh results with regard to the results of the Cartesian meshes. In this example the concentration of the nodes is made in the dielectric.

Figure6 shows the output form in the frequency domain of the cavity for an orthogonal curvilinear mesh of 120 nodes. The output is calculated as explained in section 3 above. The pick corresponds to the resonant frequency of the dominant mode TE<sub>110</sub>.

Concerning the execution time for the orthogonal curvilinear mesh and the non-uniform Cartesian mesh, it can be approximately examined through the number of iterations used in each case.

Lets compare the cases where both methods give lowest error possible that is to say CNU(20x24) for the non uniform Cartesian mesh and Cv(10x12) for the curvilinear orthogonal mesh (table1). For the CNU (20x24) the time step is  $\Delta t_1 = 1.39ps$  and for the Cv(10x12) the time step  $\Delta t_2 = 1.087ps$ . If the total number of iterations required in the case of CNU(20x24) is  $N_1$ , for Cv(10x12) the total number of iterations would be  $N_2 = N_1 \Delta t_1 / \Delta t_2$  that is to say  $N_2 = 1.279N_1$ . As can be seen, the curvilinear mesh allowed an improvement of the result by decreasing the error to 0.002%, but at the expense of number of iterations. However, since the number of arithmetic operations per node, say P, is the same in both meshes therefore the total number of operations in each case is  $P_1 = 480 \times N_1 \times P$  for the CNU(20x24) and  $P_2 = 120 \times 1.279N_1 \times P$  for the Cv(10x12). The calculation gives  $P_2 = 153.6N_1 \times P$  or  $P_2 = 0.32P_1$ . As can be seen, there is a substantial saving in the overall execution time when using the curvilinear orthogonal mesh.

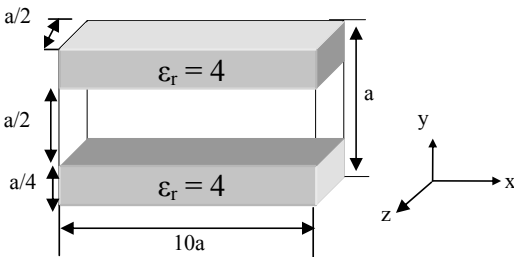


**Figure.3-** Resonant cavity with two layers of dielectric (a=7.112mm)

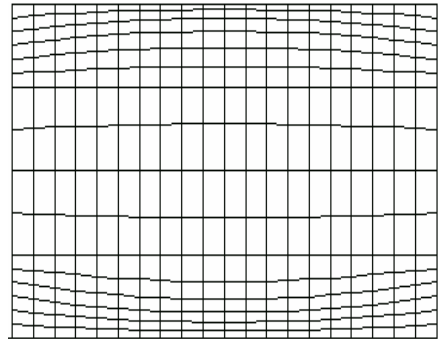


**Figure -4** Generated mesh 10X8 in the (x, y) plan

**Table1:** TLM results for different types of meshes

Type of meshes	Number of nodes	Time step ( $\Delta t$ )	TLM frequency (GHz)	Error%
*CU (40x4)	160	2.965ps	15.480	-6.72
*CU (400x40)	16000	0.2965ps	16.584	-0.07
CNU (10X6)	60	4.8141ps	16.485	-0.662
CNU (10x8)	80	3.83ps	16.648	+0.32
*CNU (10x12)	120	2.779ps	16.584	-0.07
*CNU (20x24)	480	1.39ps	16.594	-0.01
Cv (10x6)	60	4.27106ps	16.545	-0.3
Cv (10x8)	80	2.1842ps	16.606	+0.066
Cv (10x12)	120	1.087ps	16.5953	+0.002

CU: Cartesian uniform mesh  
 CNU: Cartesian non-uniform mesh  
 Cv: Curvilinear mesh  
 \*Analytical result  $f = 16.595$  GHz.  
 \*: results given by [Trenkic, V et al, 1995]



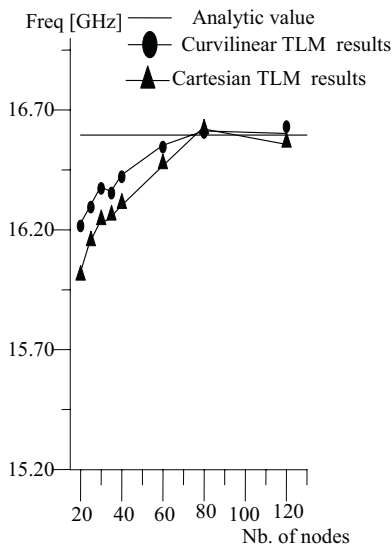


**Figure.5** Frequency variation versus number of nodes for a cavity with two layers of dielectric

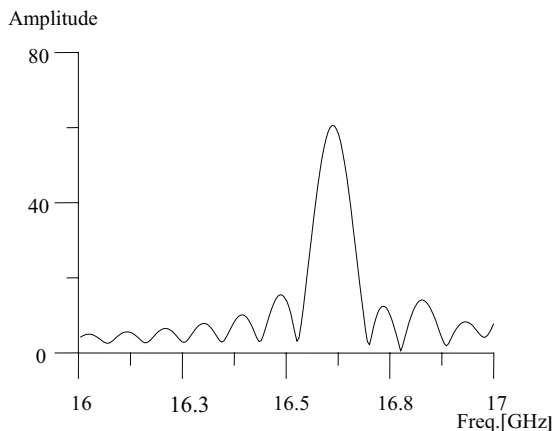


**Figure.6-** Frequency response of a resonant cavity with two layers of dielectric.

#### 4.2. Cavity With One Layer Of Dielectric In The Middle:

The problem presented in this section is the cavity shown in figure7 studied in [Akhtarzad, S et al, 1975]. It contains one layer of dielectric ( $\epsilon_r = 16$ ) in the middle. The resonance frequency of the dominant mode TE<sub>101</sub> is evaluated. The dimensions of the cavity are as follows as given in [Akhtarzad, S et al, 1975]:

Length  $a = 71.12\text{mm}$ , height  $b = 21.336\text{mm}$ , width  $c = 26.67\text{mm}$ , dielectric width  $t = 17.78\text{mm}$ ,  $\epsilon_r = 16$ .

For this problem there is no propagation in the  $y$ -direction, therefore one surface only is used in the  $y$ -direction. The excitation is done in the  $y$ -direction. The input and output nodes are taken in the dielectric.

Figure8 shows a sample of a generated mesh in the  $(x, z)$  plane for this problem. Here again, one can notice the curvature of the lines and the variation of their spacing in the dielectric layer and this is due to the presence of the dielectric. Figure9 shows how nodes are distributed in the mesh.

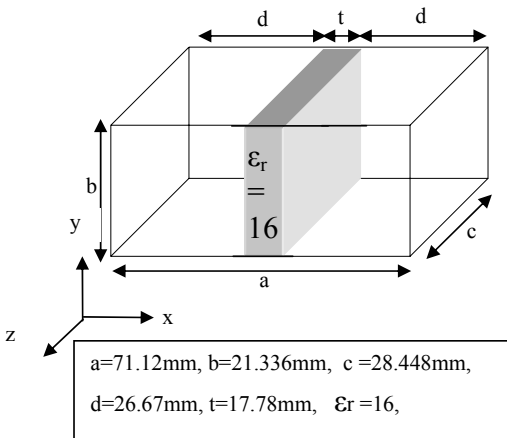
Table2 shows the results obtained for the resonant frequency of the dominant mode TE<sub>101</sub> for different types of meshes. From this table, it is clear that, for this example also, the curvilinear mesh gives better results than the Cartesian mesh. For instance, for a cartesian non-uniform mesh of 300 nodes an error of 0.4% is obtained, while for the curvilinear mesh of 280 nodes

the error is reduced to 0.028% but the time step decreases slightly. However this reduction of the time step is negligible with regard to the appreciable improvement of the result. It is worth noting, that for a uniform cartesian mesh of 7000 nodes, an error of 0.26% is obtained and this show the usefulness of the curvilinear mesh.

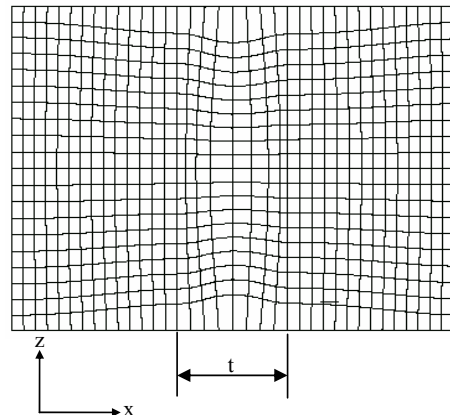
In this example, also, an investigation has been made on the convergence to the theoretical value of the different numerical results. These are shown in Figure10 that represents the variation of the frequency versus the number of nodes for the orthogonal curvilinear meshes and the non-uniform meshes. Again, in this case, one can notice the rapid convergence to the theoretical result of the curvilinear mesh results.

Figure11 shows the output form in the frequency domain of the cavity using a curvilinear mesh of 180 nodes. The output is calculated as explained in section 3 above.

Concerning the overall execution time for this case, the same approach can be used as for the precedent example. Here again, we consider the meshes, which give the best results. From table2, CNU(10+10+10)x10 mesh gives an error of 0.4% with a time step of  $\Delta t_1 = 6.197ps$  whereas Cv(10+8+10)x10 gives an error of 0.028% with a time step of  $\Delta t_2 = 5.678ps$ . The number of iterations  $N_2$  of the curvilinear mesh Cv(10+8+10) is given by  $N_2 = 1.09N_1$  where  $N_1$  is the number of iterations of the non-uniform Cartesian mesh CNU(10+10+10)x10. Here, one can notice a slight increase of the number of iterations in the case of the curvilinear mesh. The total number of operations for each case is  $P_1 = 300 \times N_1 \times P$  for the CNU mesh and  $P_2 = 280 \times N_2 \times P$  or  $P_2 = 305.2 \times N_1 \times P$  for the Cv mesh. Hence  $P_2 = 1.017P_1$ . Here, we notice a slight increase of a number of operations in the case of the orthogonal mesh but the error is drastically decreased from 0.4% to 0.028%. For the Cv(5+4+5)x10 mesh which gives an error slightly better than CNU(10+10+10)x10, the number of operations is  $P_2 = 0.56P_1$ . Here there is a significant saving in the overall execution time.



**Figure.7-** Resonant cavity with a dielectric layer in the middle



**Figure.8-**Generated surface with surface With  $10 \times (7+4+7)$  nodes

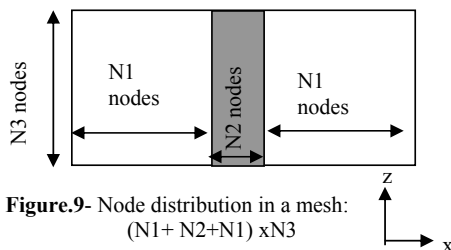


**Table2.** TLM results for different types of meshes

Mesh type	Number of nodes	Frequency TLM (GHz)	Time step ( $\Delta t$ )	Error %
CNU (5+5+5) x10	150	1.72	7.95345	-0.807
CNU (4+10+4) x10	180	1.7173	8.31804	-0.963
CNU. (7+5+7) x10	190	1.7234	7.21619	-0.611
CNU (5+10+5) x10	200	1.7209	7.95345	-0.755
CNU (10+10+10) x10	300	1.727	6.197	-0.4
Cv. (5+4+5) x10	140	1.7285	7.46	-0.31
Cv. (7+4+7) x10	180	1.731	6.87307	-0.173
Cv (10+8+10) x10	280	1.7345	5.6779	+0.028
*Cartesian uniform mesh	7000	1.7314	---	0.26

CU: Cartesian uniform mesh  
 CNU: Cartesian non uniform mesh  
 Cv: Curvilinear mesh  
 \*Analytical result  $f=1.734$  GHz.  
 \*: values given in [Akhtarzad, S et al, 1975]. The author does not give the time step.

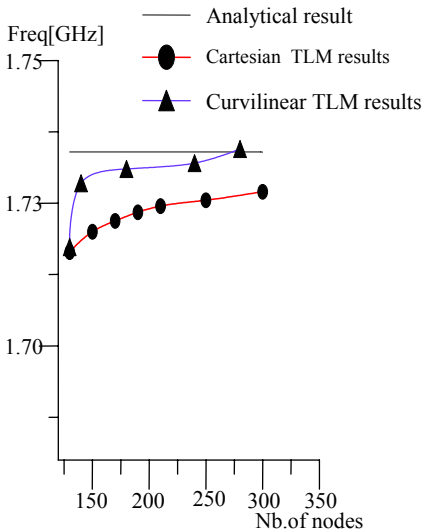


**Figure.10** Frequency variation versus number of nodes for cavity with dielectric in the middle

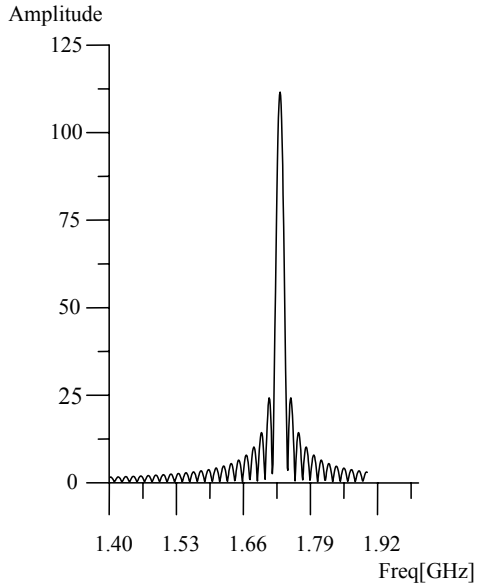


**Figure.11** Frequency response of a cavity with a dielectric in the middle.

#### 4. CONCLUSION

In this article, it is shown that the use of orthogonal curvilinear meshes in TLM yields better results with fewer nodes than the conventional cartesian meshes. The reduction of number of nodes implies the reduction in the execution time and the storage capacity.

#### REFERENCES

1. Akhtarzad, S., and Johns, P.B. J, 1975, "Three dimensional transmission line matrix to compute analysis of micro strip resonators", IEEE transactions on microwave theory and techniques.
2. Al – Mukhtar, D. A., and Sitch, J.E., "Transmission-line matrix with irregularly graded space", IEE proceedings, volume 128, Pt. H, N0 6, pages 299-305, December 1981.
3. Christopoulos, C. 1995, "The transmission -line modeling method TLM", Oxford University Press, Oxford OX2 6DP.
4. Johns, P.B., Beurle, R.L., 1971, "Numerical solution of 2-dimensional scattering problem using a transmission –line matrix", IEE proceedings, volume118, number 9, pages 1203-1208.
5. Johns, P.B., 1972, "Application of the transmission –line matrix method to homogeneous waveguides of arbitrary cross-section", IEE proceedings, volume119, number 8, pages 1086-1091.

6. Meliani, H., 1987, "Mesh generation in TLM", Ph.D Thesis, University of Nottingham, England.
7. Meliani,H., Johns, P.B., de Cogan, D., 1988 " The use of orthogonal curvilinear meshes in TLM models", International Journal of Numerical Modelling: Electronics Networks, Devices, And Fields, Vol.1, pp. 221-238.
8. Meliani, H., de Cogan,D., and Djebbar, J. A., 2000, "Report on the orthogonal curvilinear mesh generation", University of Blida , Algeria.
9. Saguet, P., Pic, E., 1981, "Le maillage rectangulaire et le changement de maille dans la methode TLM en deux dimensions", Electronic Letters, Volume 18, N0 5 pages 222-224.
10. Trenkic, V., Christopoulos,C., Trevor, C., and Benson, M., 1995, "A graded symmetrical super-condensed node for the tlm method", IEEE Transactions on Microwave theory and techniques, Volume 43, N0 6.